Journal of Materials Chemistry A

Accepted Manuscript

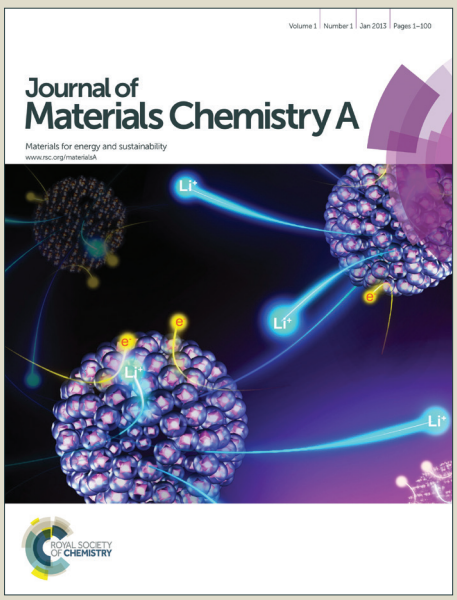

ROYAL SOCIETY OF CHEMISTRY

www.rsc.org/materialsA

Cite this: DOI: 10.1039/c0xx00000x

www.rsc.org/xxxxxx

ARTICLE TYPE

Large-scale, flexible and high-temperature resistant ZrO_2/SiC ultrafine fibers with radially gradient composition

Yingde Wang,*[a] Cheng Han,[a] Dechuan Zheng[a] and Yongpeng Lei*[b,c]

Received (in XXX, XXX) Xth XXXXXXXXX 20XX, Accepted Xth XXXXXXXXX 20XX

DOI: 10.1039/b000000x

A novel ZrO_2/SiC ultrafine fiber with radially gradient composition was prepared by a simple electrospinning technique combined with subsequent thermal treatment. The as-prepared ZrO_2/SiC fibers were analyzed by a combination of characterizations. It was found that the content of Zr was gradually degressive from the surface to the inside of the ZrO_2/SiC fiber. The gradient composition was *in situ* formed during maturation rather than subsequent pyrolysis process. The gradient compositional ZrO_2/SiC fibers with different crystalline structures were obtained by pyrolysis in Ar at different temperatures. The gradient ZrO_2 composition endows the fabricated fibers with better high-temperature stability (> 1800 °C) and much superior erosion resistance over normal SiC fibers and ZrO_2/SiC composite fibers without gradient composition. Combining the low thermal conductance of ZrO_2 with the excellent infrared heat radiation interference ability of SiC, the radially gradient fibers may have potential applications in thermal insulation systems and some other rigorous environments.

Introduction

Owing to easy processability, tailored composition and structure, polymer-derived ceramics (PDCs) routes present distinct advantages over other techniques in preparing all kinds of complicated non-oxide ceramics such as SiC,[1] SiCN,[2,3] SiBCN,[4] BN[5-7] and so on. It is worth mentioning that SiC has recently attracted more and more attentions not only due to its high-temperature stability, good corrosion resistance and excellent thermal conductivity,[8,9] but also because of its semiconductor property as photoelectric devices showing wide applications in harsh environments.[10-12]

However, when used in high temperature condition, polymer-derived SiC fiber could be oxidized with an amorphous SiO_x or SiO_xC_y outer layer, resulting in low performance of the fiber.[13,14] Generally, the adoption of surface coating is an effective way to prevent the damage of matrix,[15,16] prepared using complicated and expensive methods such as chemical vapor deposition (CVD),[17] atomic layer deposition (ALD)[18] and so on. Unfortunately, the obvious interface could induce weak junction under harsh environments, such as high temperature, strong corrosion, etc. Thus *in situ* formation of functional surface layers seems to be particularly interesting and meaningful.[19,20] It is noteworthy that controlling thermal treatment before calcination induces a maturation process in which low-molecular-mass additives bleed out from the bulk material. Subsequent calcination generates a gradient inorganic structure towards the surface without obvious interface. In a similar method, Yu *et al.* fabricated the TiO_2/SiO_2 composite fiber with smooth surface using polycarbosilane (PCS) and tetrabutyl titanate as raw materials.[21]

In the past decade, the electrospinning technique has been proved to be a low-cost, simple and continuous process for large-scalely fabricating of sub-micrometer and nano-meter fibers with controllable diameters, composition and well-defined morphologies.[22-26] However, investigations based on the combination of electrospinning and PDCs are limited,[27-30] not to mention the ceramic fibers with radially gradient composition.

In our present work, we illustrate the fabrication of a novel gradient compositional ZrO_2/SiC fiber *via* electrospinning of the precursor containing zirconium *n*-butoxide ($Zr(OC_4H_9)_4$) as low-molecular-mass additives and PCS as SiC precursor, followed by maturation and subsequent pyrolysis. During maturation, the as-prepared fibers exhibited a gradient structure from the surface towards the inside center. The gradient compositional ZrO_2/SiC fibers with ZrO_2 surface have much better high-temperature stability and erosion resistance over normal SiC fibers and ZrO_2/SiC composite fibers.

Experimental

Materials: PCS was obtained from National University of Defense Technology, China. $Zr(OC_4H_9)_4$ was purchased from Shanghai Shengzhong Co.Ltd., China. All organic solvents were purchased from Changsha Huihong Co.Ltd., China, and used without purification. High purity argon was purchased from Changsha Jingxiang Co.Ltd., China.

Electrospinning: The preparation of large-scale as-spun fibers is schematically illustrated in Fig. 1. The spinnable solution (PCSZ) was prepared *via* mixing PCS, $Zr(OC_4H_9)_4$ and xylene, followed by vigorously stirring for 6 h. After sonicating for another 1 h, the homogenous solution was loaded in several 10 mL plastic syringes and subsequently placed into our self-designed multi-

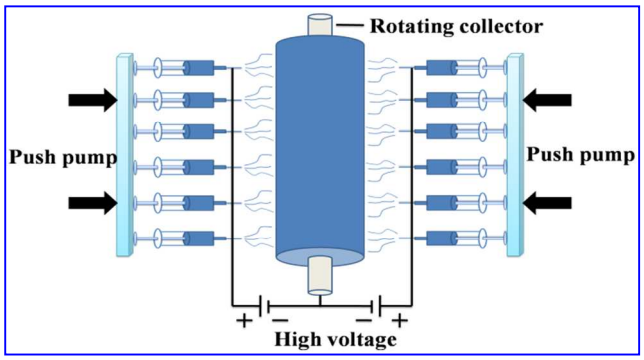

Fig. 1 Schematic illustration of large-scale electrospinning process.

needle electrospinning setup. A high voltage of 20 kV was applied between the stainless steel nozzle and rotating mental collector with a distance of 20 cm. The as-spun $Zr(OC_4H_9)_4$/PCS fibers were collected on an aluminium foil.

Preparation of radially gradient compositional ZrO_2/SiC fibers: The as-spun fibers were maturated in 120 ℃ for 100 h to make $Zr(OC_4H_9)_4$ bleed out from the fibers. After that, the maturated fibers mat was cured at 200 °C for 1 h in air (0.5 °C/min) and then pyrolysed in a tubular furnace at different temperatures for 2 h under argon atmosphere. After cooling to ambient temperature, the radially gradient compositional ZrO_2/SiC ultrafine fibers (denoted as GZS fibers) was obtained. As comparative experiments, ZrO_2/SiC composite fibers and SiC fibers (denoted as ZS fibers and S fibers, respectively) were also fabricated in a similar way as described above, but without maturation treatment.

Characterization: FTIR spectra were collected on a Nicolet Avatar 360 (USA) instrument on samples pressed as KBr pellets. X-ray diffraction (XRD) was conducted using Siemens D-5005 (Germany) with Cu Kα radiation. The x-ray photoelectron spectroscopy (XPS) analysis was recorded in a VG ESCALAB MKII instrument (USA) with Al Kα excitation. The morphological features and chemical compositions were analyzed with a field-emission scanning electron microscope (FE-SEM, JEOL-6360LV, Japan) equipped with an energy dispersive spectrometer (EDS). High-resolution transmission electron microscope (HRTEM) images were obtained using a Philips CM200 (Netherlands) operating at 200 kV. Depth profiles of GZS ultrafine fibers were measured by Auger electron spectroscope (AES) with a PHI-700 analyzer. The high-temperature stability was investigated by annealing the mat at 1800 °C in Ar atmosphere. The erosion resistance was investigated by soaking in NaOH aqueous solution (1 M, 30 min).

Results and Discussion

In order to understand the nature of the precursor solution, FTIR spectra of PCS, $Zr(OC_4H_9)_4$ and PCSZ were recorded (Fig. S1). There existed no covalent bond between $Zr(OC_4H_9)_4$ and PCS in ambient conditions. Only when the quantity of $Zr(OC_4H_9)_4$ in the precursor was fixed at 20 wt%, good spinnability of the polymer blend can be obtained. More $Zr(OC_4H_9)_4$ will lead to difficulty in electrospinning such as the incidental block of the syringe needle or the unevenness of spun fibers. The as-spun fibers mat with large area (30 × 60 cm^2) fabricated by our self-designed multi-needle electrospinning setup is given in Fig. S2. Fig. 2a shows a typical SEM image of the as-spun ultrafine fibers mat. The fibers are relatively uniform with a diameter of 3~4 μm. The diameter can be controlled by adjusting electrospinning parameters such as solution concentration, accelerating voltage, nozzle-collector distance and solution feeding rate. The surface of the gradient fiber (Fig. 2b) is very smooth, without any noticeable flaws. The XRD patterns of ZrO_2/SiC ultrafine fibers pyrolysed under different temperatures are shown in Fig. 2c. Both the crystal sizes of SiC and ZrO_2 became larger when temperature rose from 1400 to 1800 °C. And we adopt the composite fibers obtained at 1400 °C as the object of study below.

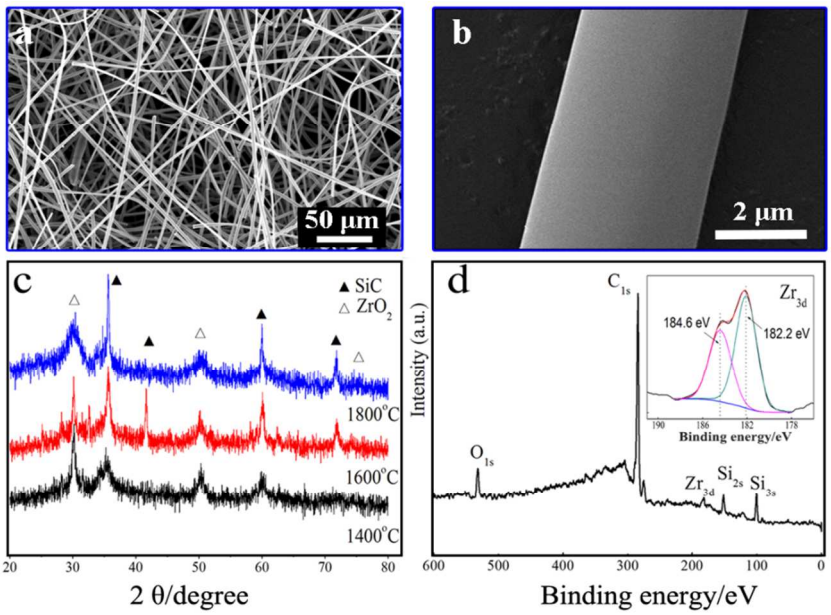

Fig.2 Typical SEM image of (a) the as-spun ultrafine fibers-based mat and (b) magnified SEM image of a single GZS fiber, (c) XRD patterns of samples pyrolysed under different temperatures and (d) XPS spectra of GSZ ultrafine fibers. The inset of (d) is high-resolution XPS spectrum of Zr_{3d}.

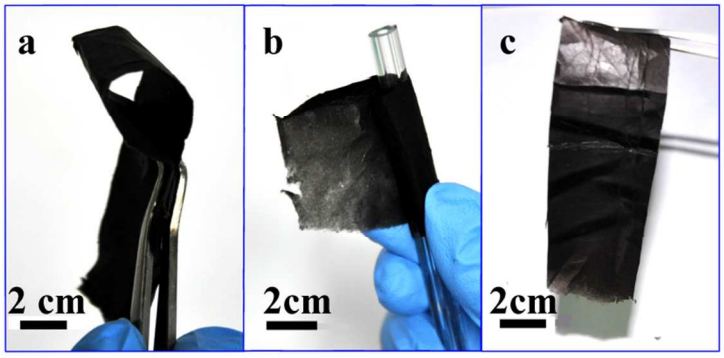

Fig. 3 Optical images of GZS fibers mat under different bending stages: (a) folded, (b) rolled up and (c) recovered after above treatments.

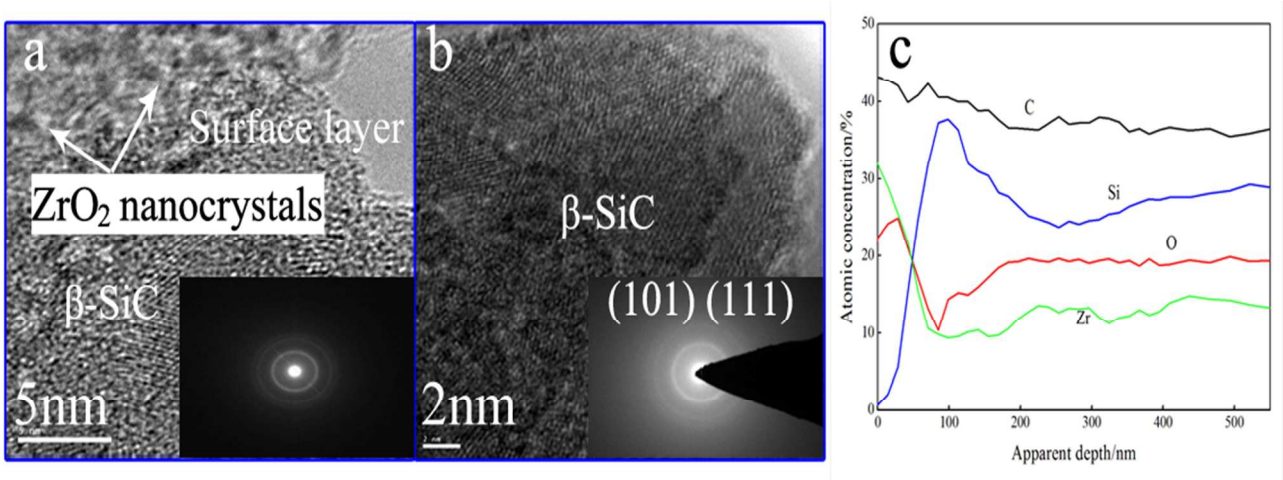

Fig. 4 HRTEM images of GZS fibers: (a) cross-section near the surface, (b) inside a single fiber and (c) AES depth profiles of C, Si, O, Zr near the surface of GZS fiber. The insets of (a, b) are corresponding crystalline diffraction rings in the SAED patterns.

To further clarify the chemical state of ZrO_2 in as-obtained fibers, XPS was performed (Fig. 2d). The Zr, O, Si and C elements were detected. The inset in Fig. 2d provides the high-resolution XPS spectrum of Zr_{3d}, appearing at a binding energy of 182.2 eV. The splitting of the Zr_{3d} doublet is about 2.4 eV, in good agreement with the literature value of the Zr^{4+} state in stoichiometric ZrO_2.[31]

The flexibility of the fibers mat is illustrated by the digital photographs of our scissored GZS fibers mat under different stages (Fig. 3). The fibers mat exhibited good flexibility after being folded and rolled up. The main factors contributed to such flexibility are that the fibers are individual and have a small diameter (Fig. 2a). Hence, they can slide against each other to lower stress concentration during bending.[30] The mat with good flexibility facilitates its practical use in sophisticated devices.

To investigate the radially gradient composition of Zr element in the prepared GSZ fibers, HRTEM and AES were recorded. The radially gradient composition is confirmed by a HRTEM image of the cross-section near the surface of an ultrafine GZS fiber (Fig. 4a). The ZrO_2 nanocrystals intensively exist in the surface layer of the fiber, indicating the direct production of a gradient composition of ZrO_2 towards the surface. Fig. 4b shows the typical microstructure of a single GZS ultrafine fiber. The highly crystalline SiC arrayed in a broad area. The corresponding (101), (111) crystal planes shown in the selected area electron diffraction (SAED) pattern (Fig. 4b inset) confirmed the formation of β-SiC phase in ultrafine GZS fibers.[32] The typical crystal of ZrO_2 is not obvious in Fig. 4b, probably because of the relatively low content of ZrO_2 inside the fiber. AES depth analysis of the fiber surface in Fig. 4c illustrates that the content of Zr near the surface decreased from 32 to 10 wt% towards the inside in 100nm. The result is consistent with the TEM analysis near the surface layer of GZS ultrafine fiber, demonstrating the radially gradient composition construction in GZS ultrafine fibers

In order to better understand the growing mechanism of the radially gradient compositional ZrO_2 during maturation, we have prepared GZS fibers mat under different maturing conditions. The SEM and EDS of surface and cross-section regions of GZS ultrafine fibers are presented in Fig. 5. Sample a and b were prepared by maturing spun ultrafine fibers under 100 °C for 30 h and 120 °C for 100 h. Number 1 and 2 indicate the measured spots of cross-section and surface, respectively.

As shown in Fig. 5a1 and a2, the content of Zr element in surface region and cross-section content is almost the same. The gradient construction is not obvious. In Fig. 5b1 and b2, the as-spun ultrafine fiber maturated under higher temperature and longer time, the Zr content in the surface and inside the ZrO_2/SiC fibers changed to be 18.85 and 9.48 wt%, respectively. These results confirm that the bleeding out of additive happened in maturing process rather than subsequent pyrolysing process. A

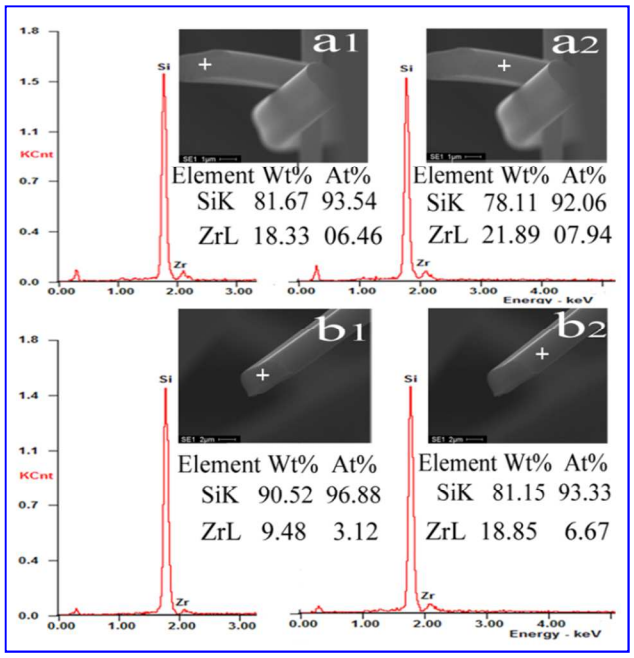

Fig.5 SEM and EDS images of GZS fibers with different maturing conditions: the spinning solution containing 20 wt% $Zr(OC_4H_9)_4$ and the maturing process was performed at (a) 120 °C, 100 h; (b) 100 °C, 30 h. Insets are element contents in cross section region (inside) (a1, b1) and surface region (a2, b2) of the GSZ fiber.

suitable maturing condition before curing of the as-spun ultrafine fibers plays a key role in the formation of gradient structure.

The tentative formation mechanism of radially gradient compositional ZrO_2/SiC fibers is schematically illustrated in Fig. 6. Controlled maturation of the as-spun fibers induced phase separation of $Zr(OC_4H_9)_4$ from PCS bulk. There are two ways that could transform $Zr(OC_4H_9)_4$ into ZrO_2 crystalline in subsequent curing and pyrolysis process, stabilizing the compositionally changed surface area. One way is that, the H_2O generated from the oxidation of Si-H bonds in PCS (eq.1) during curing induced the hydrolyzation of $Zr(OC_4H_9)_4$ into Zr-OH^- (eq.2) and subsequent pyrolysis formed crystallized ZrO_2 (eq.3).

$$2\,Si-H+O_2 \longrightarrow Si-O-Si+H_2O \quad (1)$$

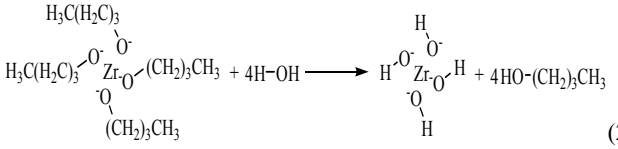

(2)

$$Zr-OH^- + {}^-HO-Zr \longrightarrow Zr-O-Zr+H_2O \quad (3)$$

The other way is that, when pyrolysed at high temperature, $Zr(OC_4H_9)_4$ could be directly transformed into ZrO_2 (eq.4) :

$$Zr(OC_4H_9)_4 \longrightarrow Zr-O-Zr+\text{volatiles} \quad (4)$$

We suppose that the force of phase separation in maturing process came from the trend to reduce the free energy of mixing.[33] When maturation was performed under an appropriate temperature, phase separation happened to reduce the free energy of the blending system,[34] just like the normally outward loss of additives components from some plastics.[19,35] Thus the zirconium compound diffused to the surface region. Diffusion is a time-consuming process, and diffusion distance depends on the temperature and time. Hence, to form gradient composition, it is necessary that the as-spun fibers be kept for enough time at appropriate temperature to make low-molecular-mass additives bleed out of the bulk fibers. The radially gradient composition could then be controlled by varying the maturing conditions through changing the temperature and holding time.

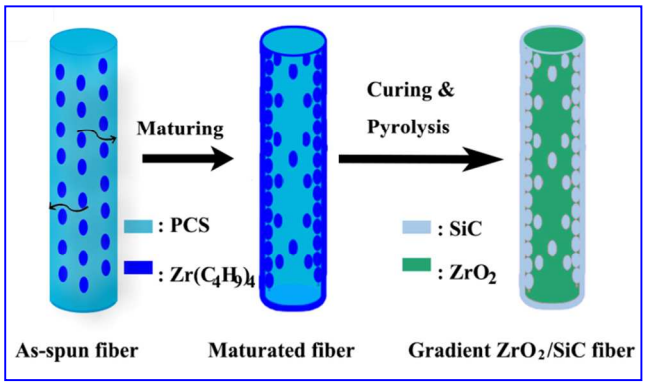

Fig. 6 Schematic illustration for the conversion of as-spun fiber into GZS fiber.

For a better understanding of the properties of as-prepared GZS fibers, the high temperature stability and erosion resistance were tested. Comparative studies were carried out using GZS fibers, ZS fibers (without maturation), and S fibers. The fractured surface of the tested fiber was recorded using SEM (Fig. 7).

As seen in Fig. 7a, after being annealed at 1800℃ in Ar for 1 h, S fibers (**a1**) are easily crashed into pieces while GZS fibers (**a2**) remain intact. The erosion resistance was investigated by immersing the fibers mat (after being calcinated at 700 ℃ in air for 10 h) in NaOH solution (1 M, 30 min). In Fig. 7b, ZS fibers (**b1**) have been extensively oxidized and bonded together whereas the morphology of the GZS fibers (**b2**) have rarely been damaged. All these results suggest that GZS fibers with surface ZrO_2 layer have much better high-temperature stability and erosion resistance over S fibers and ZS fibers. It is important to point out that, due to the synergetic effect between SiC and metal oxide, such heterogeneous phase fibers mat with good flexibility provides great potential in thermal insulator, energy,[36] catalysts,[37,38] sensors,[39] filtration,[40] and many other applications.

Conclusions

We have demonstrated a strategy for the fabrication of large-scale, flexible ZrO_2/SiC ultrafine fibers with radially gradient composition *via* electrospinning of $Zr(OC_4H_9)_4$ and PCS, followed by maturation and subsequent high-temperature pyrolysis. The gradient compositional ZrO_2 construction was *in situ* formed and suitable maturing played a key role in the fabrication of gradient construction. With a ZrO_2 surface layer,

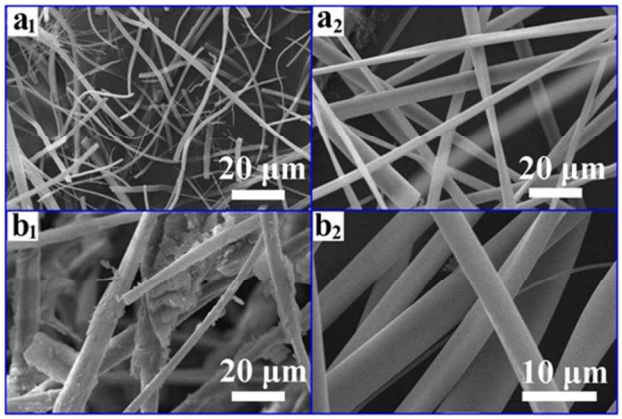

Fig.7 SEM images of fibers treated under different conditions: (a1) S and (a2) GZS after being annealed in air (1800°C, 1 h); (b1) ZS and (b2) GZS micrographs, which had been calcinated in air (700 °C, 10 h) and subsequently immersed in NaOH solution (1 M, 30 min). S, ZS and GZS represent SiC fiber, ZrO_2/SiC fiber (without maturation) and gradient compositional ZrO_2/SiC fiber, respectively.

the GZS ultrafine fibers show much better high-temperature stability and erosion resistance. We believed that, because of the synergetic effect between SiC and the metal oxides, this type of ultrafine fibers mat should have potential application in the field of thermal insulators, catalysts, gas sensors in harsh conditions such as corrosive and high temperature environments, etc.

Acknowledgments

The work was financially supported by National Natural Science Foundation of China (No.51173202 and No.51203182), Hunan Provincial Natural Science Foundation of China (No. 13JJ4009), Aeronautical Science Foundation of China (No. 2013ZF88007), State Key Laboratory for Mechanical Behavior of Materials, Xi'an Jiaotong University (No. 20131304), State Key Laboratory for Modification of Chemical Fibers and Polymer Materials, Dong Hua University (No. LK1207), Key Laboratory of Advanced Textile Materials and Manufacturing Technology (Zhejiang Sci-Tech University), Ministry of Education (No. 2013002), Aid program for Science and Technology Innovative Research Team in Higher Educational Institutions of Hunan Province and Aid Program for Innovative Group of National University of Defense Technology. We thank Dr. Yanzi Gou's helpful discussions and we also appreciate the reviewers' kind comments.

Notes and references

[a] *Science and Technology on Advanced Ceramic Fibers and Composites Laboratory, National University of Defense Technology, 109 Deya Road, Changsha 410073, PR China. Fax:* 86 73184575118*; Tel:* 86 731 84575118*; E-mail: wyd502@163.com*

[b] *State Key Laboratory for Mechanical Behavior of Materials, Xi'an Jiaotong University, Xi'an 710049, PR China*

[c] *College of Basic Education, National University of Defense Technology, Changsha 410073, PR China; E-mail: lypkd@163.com*

1 H. Wang, X. D. Li, J. S. Yu and D. P. Kim, *J. Mater. Chem.*, 2004, **14**, 1383.

2 G. Mera, A. Navrotsky, S. Sen, H.-J. Kleebe and R. Riedel, *J. Mater. Chem. A*, 2013, **1**, 3826.

3 K. Jian, Z. H. Chen, Q. S. Ma, W. W. Zheng and H. F. Hu, *Ceram. Int.*, 2007, **33**, 905

4 Y. Tang, J. Wang, X. D. Li, Z. F. Xie, H. Wang, W. H. Li and X. Z. Wang, *Chem. Eur. J.*, 2010, **16**, 6458.

5 Y. P. Lei, Y. D. Wang, Y. C. Song, H. Wang, Z. F. Xie and C. Deng, *Mater. Lett.*, 2011, **65**, 1111.

6 Y. P. Lei, Y. D. Wang, Y. C. Song, H. Wang, Z. F. Xie and C. Deng, *Mater. Lett.*, 2011, **65**, 157.

7 Y. P. Lei, Y. D. Wang and Y. C. Song, *Ceram. Int.*, 2012, **38**, 271.

8 J. Y. Fan, X. L. Wu and P. K. Chu, *Prog. Mater. Sci.*, 2006, **51**, 983.

9 K. Zekentes and K. Rogdakis, *J. Phys. D: Appl. Phys.*, 2011, **44**, 133001.

10 H. T. Wang, L. Lin, W. Y. Yang, Z. P. Xie and L. N. An, *J. Phys. Chem. C*, 2010, **114**, 2591.

11 R. B. Wu, K. Zhou, J. Wei, Y. Z. Huang, F. Su, J. J. Chen and L. Y. Wang, *J. Phys. Chem. C*, 2012, **116**, 12940.

12 J. J. Niu and J. N. Wang, *J. Phys. Chem. B*, 2007, **111**, 4368.

13 H. L. Hou, C. L. Dong, L. Wang, F. M. Gao, G. D. Wei, J. J. Zheng, X. M. Cheng, B. Tang and W. Y. Yang, *CrystEngComm.*, 2013, **15**, 2002.

14 H. Kodama, H. Sakamoto and T. Miiyoshi, *J. Am. Ceram. Soc.*, 1989, **72**, 551.

15 L. Shen , B. J. Tan, W. S. Willis, F. S. Galasso and S. L. Sui, *J. Am. Ceram. Soc.*, 1994, **77**, 1011.

16 D. F. Lii, J. L. Huang, L. J. Tsui and S. M. Lee, *Surf. Coat. Tech.*, 2002, **150**, 269.

17 N. I. Baklanova, T. M. Zima, A. I. Boronin, S. V. Kosheev, A. T. Titov, N. V. Isaeva, D. V. Graschenkov and S. S. Solntsev, *Surf. Coat. Tech.*, 2006, **201**, 2313.

18 B. Díaz, E. Härkönen, J. Światowska, V. Maurice, A. Seyeux, P. Marcus and M. Ritala, *Corros. Sci.*, 2011, **53**, 2168.

19 A. Perovic and D. K. Murti, *J. Appl. Polym. Sci.*, 1984, **29**, 4321.

20 T. Ishikawa, H. Yamaoka, Y. Harada, T. Fujii and T. Nagasawa, *Nature*, 2002, **416**, 64.

21 Y. X. Yu, Y. D. Guo, X. Cheng and Y. Zhang, *J. Mater. Chem.*, 2009, **19**, 5637.

22 M. Shang, W. Z. Wang, S. M. Sun, E. P. Gao, Z. J. Zhang, L. Zhang and R. O'Hayreb, *Nanoscale*, 2013, **5**, 5036.

23 B. Sun, Y. Long, Z. Chen, S. Liu, H. Zhang, J. Zhang and W. Han, *J. Mater. Chem. C*, 2014, **2**, 1209.

24 Y.Yu, L. Gu, C. B. Zhu, P. A. V. Aken and J. Maie. *J. Am. Chem.Soc.*, 2009, **131**,15984.

25 H. Dai, J. Gong, H. Kim and D. Lee, *Nanotechnology*, 2002, **13**, 674.

26 D. Li and Y. N. Xia, *Adv. Mater.*, 2004, **16**, 1151.

27 D. T. Welna, J. D. Bender, X. Wei, L. G. Sneddon and H. R. Allcock, *Adv. Mater.*, 2005, **17**, 859.

28 J. Wilfert, R.V. Hagen, R. Fiz, M. Jansen and S. Mathur, *J. Mater. Chem.*, 2012, **22**, 2099.

29 29 V. Salles, S. Bernard, A. Brioude, D. Cornu and P. Miele, *Nanoscale*, 2010, **2**, 215.

30 Y. X. Yu, Y. Chen and L. N. An, *Int. J. Appl. Ceram. Technol.*, DOI:10.1111/ijac.12081.

31 Y. H. Pan, Y. Gao, D. D. Kong, G. D. Wang, J. B. Hou, S. W. Hu, H. B. Pan and J. F. Zhu, *Langmuir*, 2012, **28**, 6045.

32 J. Q. Hu, Y. Bando, J. H. Zhan and D. Golberg, *Appl. Phys. Lett.*, 2004, **85**, 2932.

33 O. Olabisi, Polymer-Polymer miscibility, *Academic Press N.Y.* 1979, chapter **2**, 3.

34 J. L.Chen and F. C. Chang, *Macromolecules,* 1999, **32**, 5348.

35 A. Perovic and P. R. Sundararajan, *Polym. Bull.*,1982, **6**, 277.

36 Y. M. He, W. J. Chen, C. T. Gao, J. Y. Zhou, X. D. Li and E. Q. Xie, *Nanoscale*, 2007, **19**, 1231.

37 A. C. Patel, S. X. Li, J. M. Yuan and Y. Wei, *Nano Lett.*, 2006, **6**, 1042.

38 J. L. Shi, *Chem. Rev.*, 2013, **113**, 2139.

39 A. C. Patel, S. X. Li, C. Wang, W. J. Zhang and Y.Wei, *Chem. Mater.*, 2007, 19, 1231.

40 F. K. Ko, Nanofiber technology: Bridging the gap between nano and macro world, in *Nanoengineered Nanofibrous Materials*, ed. S. Guceri et al. Kluwer Academic Publishers. 2004, 1-18.

I

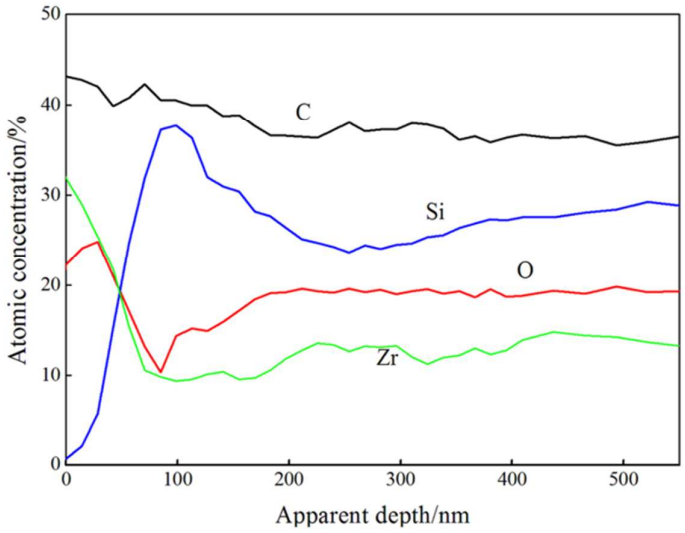

II

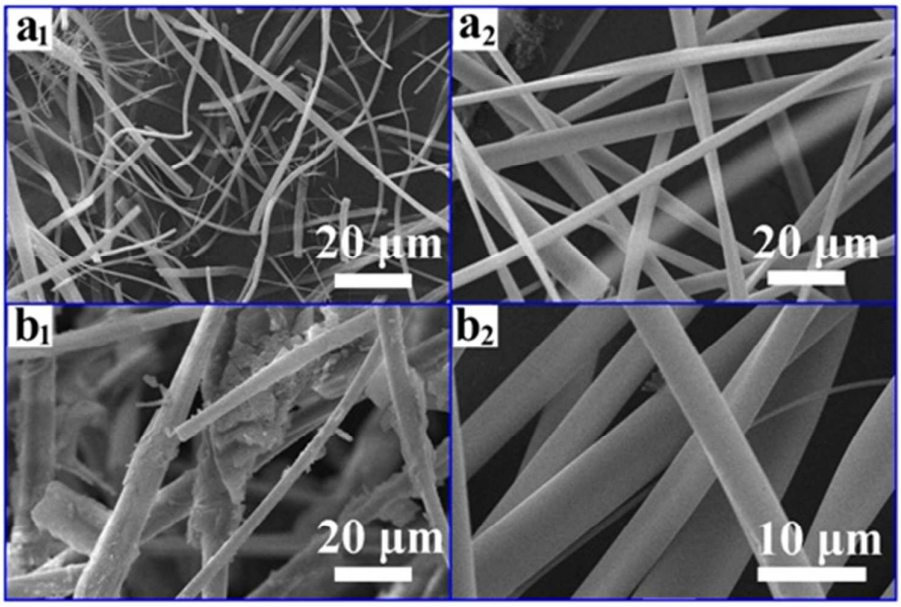

I: AES depth profiles of C, Si, O, Zr near the surface of as-prepared ZrO_2/SiC fiber with radially gradient composition.

II: SEM images of fibers treated under different conditions: (a1) S and (a2) GZS after being annealed in air (1800°C, 1 h); (b1) ZS and (b2) GZS micrographs, which had been calcinated in air (700 °C, 10 h) and subsequently immersed in NaOH solution (1 M, 30 min). S, ZS and GZS represent SiC fiber, ZrO_2/SiC fiber (without maturation) and gradient compositional ZrO_2/SiC fiber, respectively.